

## **Supplementary Information**

### Ductile deformation mechanism in semiconductor $\alpha$ -Ag<sub>2</sub>S

Guodong Li <sup>\*,1,2</sup>, Qi An <sup>3</sup>, Sergey I. Morozov <sup>4</sup>, Bo Duan <sup>1</sup>, William A. Goddard III <sup>5</sup>, Qingjie Zhang <sup>\*,1</sup>, Pengcheng Zhai <sup>1</sup>, and G. Jeffrey Snyder <sup>\*,2</sup>

<sup>1</sup>State Key Laboratory of Advanced Technology for Materials Synthesis and Processing, Wuhan University of Technology, Wuhan 430070, China.

<sup>2</sup>Department of Materials Science and Engineering, Northwestern University, Evanston, Illinois 60208, USA.

<sup>3</sup>Department of Chemical and Materials Engineering, University of Nevada Reno, Reno, Nevada 89557, USA

<sup>4</sup>Department of Computer Simulation and Nanotechnology, South Ural State University, Chelyabinsk 454080, Russia

<sup>5</sup>Materials and Process Simulation Center, California Institute of Technology, Pasadena, California 91125, USA.

\*Corresponding authors: jeff.snyder@northwestern.edu; zhangqj@whut.edu.cn; guodonglee@whut.edu.cn

**Deformation mechanism of  $\alpha$ -Ag<sub>2</sub>S under pure shear load along the (100)[00-1] slip system**

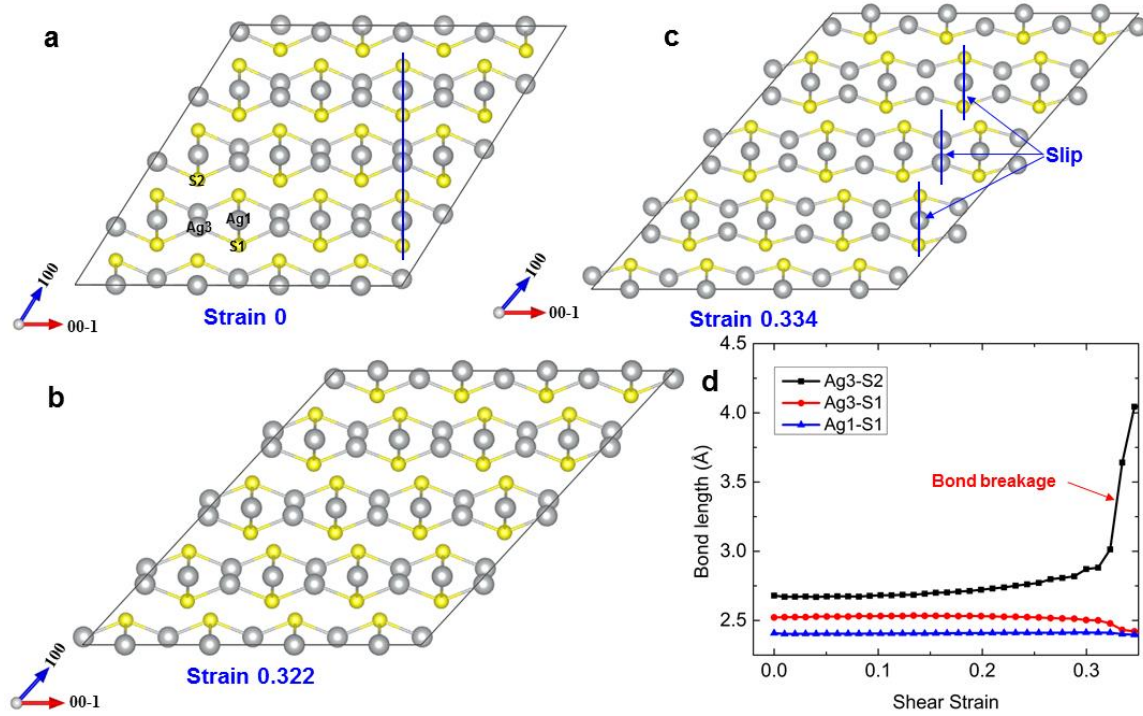


**Fig. S1 Deformation mechanism of  $\alpha$ -Ag<sub>2</sub>S under pure shear load along the (100)[00-1] slip system.** (a) The intact structure. (b) Atomic structure at 0.322 shear strain, before the structural failure. (c) Atomic structure at failure strain of 0.334. (d) The typical bond lengths (Ag3-S2, Ag3-S1, and Ag1-S1) as a function of shear strain. The breakage of the Ag3-S2 bond leads to the slip between stacked Ag-S frameworks, giving rise to the failure of  $\alpha$ -Ag<sub>2</sub>S for shearing along (100)[00-1].

Deformation mechanism of  $\alpha$ -Ag<sub>2</sub>S under uniaxial tensile load along the [100] direction

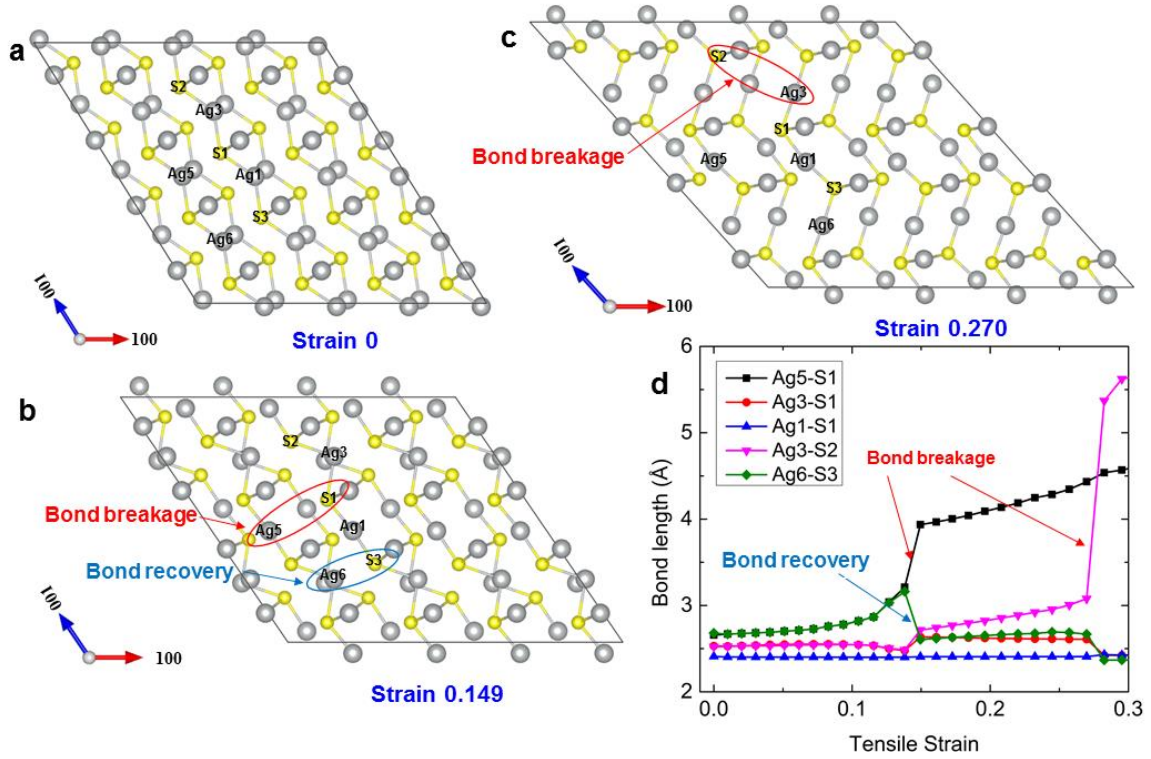


**Fig. S2 Deformation mechanism of  $\alpha$ -Ag<sub>2</sub>S under uniaxial tensile load along the [100] direction.** (a) The intact structure. (b) Atomic structure at 0.149 tensile strain, at which the Ag5–S1 bond breaks while the Ag6–S3 bond recovers. (c) Atomic structure at failure strain of 0.270. (d) The typical bond lengths (Ag5–S1, Ag3–S1, Ag1–S1, Ag3–S2, and Ag6–S3) as a function of tensile strain. The softening and breakage of the Ag5–S1 bond leads to the structural softening from 0.104 to 0.149 tensile strain (Fig. 2a). While recovery of the Ag6–S3 bond further couples the stacked Ag-S frameworks (Fig. S2b), leading to the plastic deformation of  $\alpha$ -Ag<sub>2</sub>S with further increasing tensile strain. At 0.27 failure strain, the breakage of the Ag3–S2 bond leads to the failure of  $\alpha$ -Ag<sub>2</sub>S along the [100] tension.

**Bond-responding response of  $\alpha$ -Ag<sub>2</sub>S under biaxial shear load along the (100)[010] system**

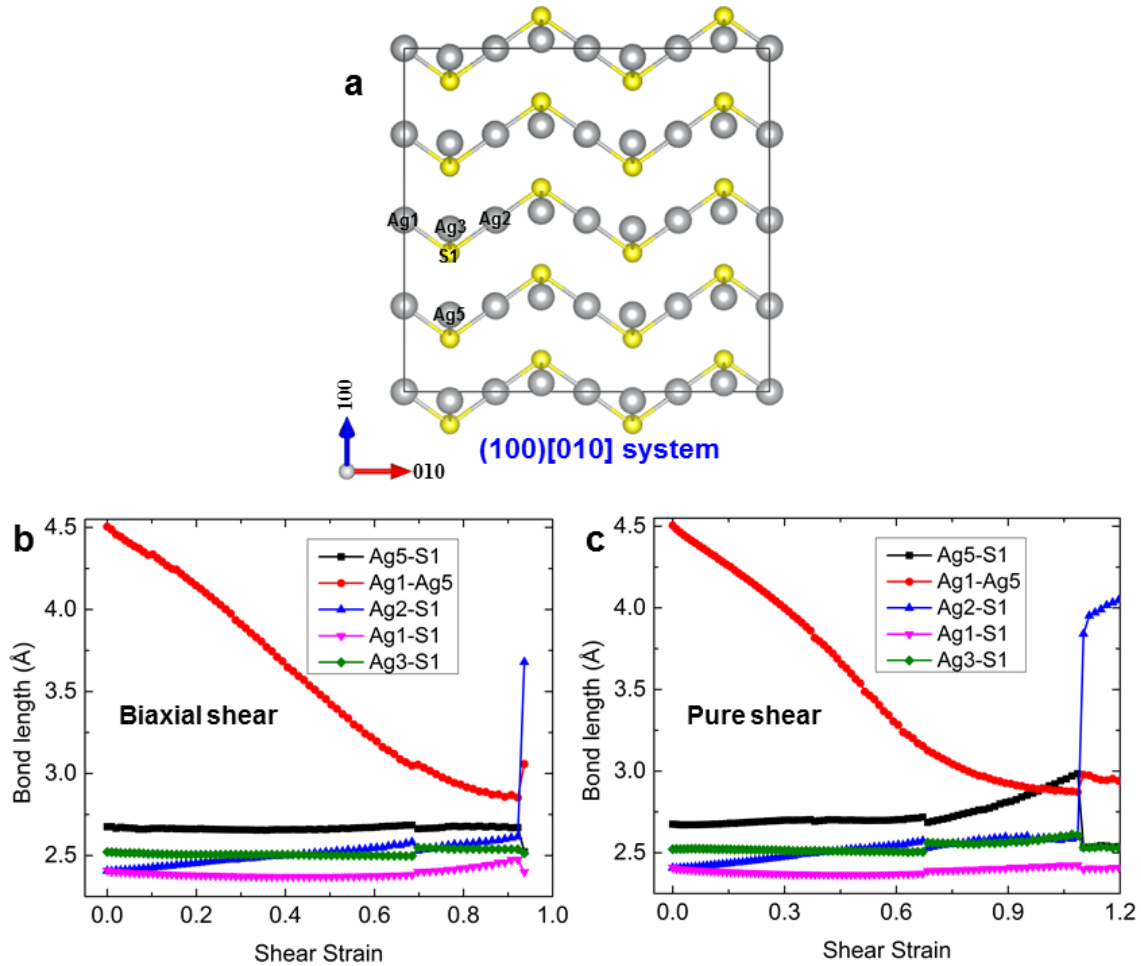


**Fig. S3 Bond-responding response of  $\alpha$ -Ag<sub>2</sub>S under biaxial shear load along the (100)[010] system.** (a) The intact atomic structure shear along (100)[010] system. (b,c) The typical bond lengths (Ag5–S1, Ag1–Ag5, Ag2–S1, Ag1–S1, and Ag3–S1) against shear strain (b) under biaxial shear load and (c) under pure shear load. Under biaxial shear and pure shear loads,  $\alpha$ -Ag<sub>2</sub>S exhibits the similar bond-responding response: The Ag1–Ag5 bond reforming strengthens the material, holding the stacked Ag–S frameworks together and remaining the structural integrity. The breakage of the Ag2–S1 bond leads to the failure. These bond-responding responses well explains the similar stress responses under biaxial shear and pure shear load, as shown in Fig. 6.

## The detailed deformation simulation setups

To simulate quasi-static mechanical loading process, we applied pure shear and uniaxial tensile deformations on  $\alpha$ -Ag<sub>2</sub>S by imposing the shear or tensile strain on a particular system while allowing structural relaxation along the other five strain components.<sup>1</sup>

To obtain stress-strain curves, a small shear strain was applied sequentially to the supercell configuration relaxed in the previous step. We predefined a 1% level of strain as the small strain increment for each deformation step. This stress – strain curve was used to obtain the ideal shear strength, and to determine the deformation modes responsible for ductility in single crystalline  $\alpha$ -Ag<sub>2</sub>S.

The biaxial shear deformation was also examined to mimic the stress conditions in Vickers indentation experiments. Here we considered a biaxial stress distribution beneath an indenter with a shear stress ( $\sigma_{xz}$ ) and a normal compressive stress component ( $\sigma_{zz}$ ). They are constrained as  $\sigma_{xz} = \sigma_{zz} \tan \phi$ , where  $\phi = 68^\circ$  is the centerline-to-face angle for a Vickers indenter.<sup>2</sup>

The residual stresses for relaxation along the other strain components both in pure shear, uniaxial tensile and biaxial shear deformations are all less than 0.1 GPa. This relaxation method has been proved to be an effective tool to shed lights on the intrinsic deformation mechanism at the atomic scale.<sup>3</sup>

## REFERENCES

1. Li, G. *et al.* Superstrengthening Bi<sub>2</sub>Te<sub>3</sub> through nanotwinning. *Phys. Rev. Lett.* **119**, 085501, (2017).
2. Li, B., Sun, H. & Chen, C. Large indentation strain-stiffening in nanotwinned cubic boron nitride. *Nat. Commun.* **5**, 4965, (2014).
3. Ogata, S., Li, J. & Yip, S. Ideal pure shear strength of aluminum and copper. *Science* **298**, 807-811 (2002).